

1 **Title: An environmental determinant of viral respiratory disease**

2 Authors:

3 Yeon-Woo Choi^{1,†}, PhD

4 Alexandre Tuel^{1,†,*}, MSc

5 Elfatih A. B. Eltahir¹, PhD

6

7 **ABSTRACT:**

8 The evident seasonality of influenza suggests a significant role for weather and climate as one of
9 several determinants of viral respiratory disease (VRD), including social determinants which
10 play a major role in shaping these phenomena. Based on the current mechanistic understanding
11 of how VRDs are transmitted by small droplets, we identify an environmental variable, Air
12 Drying Capacity (ADC), as an atmospheric state-variable with significant and direct relevance to
13 the transmission of VRD. ADC dictates the evolution and fate of droplets under given
14 temperature and humidity conditions. The definition of this variable is rooted in the Maxwell
15 theory of droplet evolution via coupled heat and mass transfer between droplets and the
16 surrounding environment. We present the climatology of ADC, and compare its observed
17 distribution in space and time to the observed prevalence of influenza and COVID-19 from
18 extensive global data sets. Globally, large ADC values appear to significantly constrain the
19 observed transmission and spread of VRD, consistent with the significant coherency of the
20 observed seasonal cycles of ADC and influenza. Our results introduce a new environmental
21 determinant, rooted in the mechanism of VRD transmission, with potential implications for

22 explaining seasonality of influenza, and for describing how environmental conditions may
23 impact to some degree the evolution of similar VRDs, such as COVID-19.

24 ¹Ralph M. Parsons Laboratory, Massachusetts Institute of Technology, Cambridge,
25 Massachusetts 02139, USA

26 † equal contribution

27 * e-mail: atuel@mit.edu

28 TEL: (617) 253-6596

29 **Main**

30 The spread of Viral Respiratory Diseases (VRDs), like influenza and COVID-19, is shaped by a
31 combination of social, biological and environmental determinants. Social determinants include
32 behavioural aspects (settlement density, mobility, personal hygiene, vaccination, social
33 distancing, etc.) that affect the transmission of the disease. Biological determinants are defined
34 here as characteristics of the pathogen itself including its response to abiotic factors, and the
35 nature of the human immune response to it. Finally, environmental determinants are defined here
36 as the set of environmental conditions that impact the intensity of the disease transmission
37 process. (For example, how much a virus tolerates extreme temperature is a biological
38 determinant, while how extreme temperature impacts the transmission of the virus is an
39 environmental determinant.) Most public policy approaches to limit the spread of VRDs
40 typically rely on manipulating social behaviours through emphasis on personal hygiene, social
41 distancing and vaccination, and COVID-19 is no exception. Still, the dynamics and average
42 prevalence of VRDs exhibit substantial variability across countries. Influenza is most widespread
43 in the mid-latitudes,¹ and in the case of COVID-19, some countries have clearly experienced
44 widespread transmission and an explosive growth in cases, while in others, the outbreak seems
45 much more constrained.²⁻⁴ It is evident that social determinants play a major role in controlling
46 transmission, especially given the success of social distancing policies implemented in response
47 to COVID-19. However, this does not necessarily imply that the environment plays no role in
48 shaping VRD spread, as highlighted by the clear seasonality of influenza in mid-latitude
49 countries.¹

50 We still do not have a definite understanding of the biological determinants of VRDs. Laboratory
51 experiments have suggested that ambient temperature and absolute humidity affected the
52 survival of several VRD pathogens,⁵⁻⁷ although the effect of temperature seems weak in the case
53 of the SARS-CoV-2 virus responsible for COVID-19⁸ (Fig. S1). High UV radiation is also
54 believed to suppress viral activity and infectivity in the case of influenza viruses⁹ and possibly
55 SARS-CoV-2.¹⁰ Additionally, evidence has emerged that viral shedding in mammals is enhanced
56 at low temperatures,¹¹ making the case for strong biological controls on VRD prevalence.
57 Yet, because VRDs are primarily transmitted by droplets exhaled by infected subjects,
58 environmental conditions may also play a major role in shaping their spread.^{12,13} Previous studies
59 have argued that cold and dry environments were conducive to the survival and transport of
60 VRD-infected droplets, unlike warm and humid environments.^{1,6} This hypothesis seems
61 supported by empirical relationships applied to country-level data,^{7,14,15,16} though in the case of
62 COVID-19 initial results suggest that weather and climate conditions may have limited effects
63 on the spread of the disease.^{17,18}
64 One important limitation of such studies is their focus on temperature or humidity as separate
65 covariates to understand or predict VRD prevalence. Different relationships are developed for
66 tropical and mid-latitude countries¹ although the physics of droplets is the same. Additionally,
67 relationships are sometimes found to be non-monotonic: in the case of COVID-19, the
68 transmission efficiency may first be enhanced as temperature and absolute humidity drop, and
69 then decline beyond a certain threshold.¹⁵ Therefore, while evidence points to some degree of
70 environmental control on VRD spread and prevalence, the lack of a consistent and physically-
71 based framework makes it all the more difficult to assess.

72 Here, we propose a new atmospheric state-variable, named Air Drying Capacity (ADC), rooted
73 in the current mechanistic understanding of how transmission takes place by small droplets.
74 ADC is defined as the rate of decrease with time of a droplet surface area, given ambient
75 temperature and humidity. As such, ADC integrates naturally the effects of both temperature and
76 humidity based on their relative roles in dictating the decrease of the droplet surface area. ADC
77 offers a consistent, physically-based framework to assess the effect of environmental conditions
78 on global and seasonal patterns of VRD prevalence.

79

80 **Methods**

81 **Droplet Theory of VRD Transmission**

82 VRDs are believed to be transmitted by droplets exhaled by infected subjects.¹⁹⁻²² The size of
83 exhaled droplets by human typically ranges from about 0.5 μm in breathing, and increases with
84 speech up to about 10 μm .²³ Larger droplets, up to 200-300 μm , can be emitted by sneezing or
85 coughing.²⁴ After emission, droplets can contaminate nearby surfaces, or disperse as aerosols and
86 may infect subjects who inhale them. This idea, first developed by Wells,²⁵ led to the
87 discrimination of “large” and “small” droplets, and has since then influenced strategies to control
88 the spread of infection according to whether the disease was thought to be transmitted primarily
89 through large or small droplets.²⁶ Droplet diameter cut-offs usually range between 5 and 10 μm ,²⁷
90 and the typical associated distance varies between 1.5 and 2m.²⁸ More recent studies have
91 shown, however, that these arbitrary droplet size cut-offs do not reflect the actual trajectories of
92 exhaled droplets. The dynamics of droplet evaporation and evolution are indeed very dependent
93 on the characteristics of the complex multiphase turbulent flow which the droplets exist in²⁹ as

94 well as background environmental conditions.¹² While influenza transmission has been shown to
 95 occur through both the large and small droplet route,²¹ at this stage, COVID-19 is still believed
 96 to be mainly transmitted by the large droplet path,³⁰ although aerosol transmission may also be
 97 possible.³¹ In any case, exhaled droplets are still the major infection route, which implies that
 98 environmental controls on droplet evaporation and disappearance may play an important role in
 99 determining the spread of the disease.

100

101 **A proposed environmental determinant: Atmospheric Drying Capacity (ADC)**

102 Droplet growth theory under given environmental conditions goes back to the pioneering work
 103 of Maxwell,³² who first posited that steady-state dynamics of spherical droplets at rest in
 104 isotropic gaseous media were controlled by the equilibrium between heat and mass exchange at
 105 their surface. Both mass and heat transfer involve ambient temperature and humidity, and are
 106 therefore strongly constrained by environmental conditions. In steady-state, mass and heat
 107 transfer exactly compensate, and one finds that the radius r of a droplet evolves according to³³:

$$108 \quad r \frac{dr}{dt} = \frac{(RH - 1)}{\left(\frac{L_v}{R_v T_a} - 1\right) \frac{L_v \rho}{K T_a} + \frac{\rho R_v T_a}{e_s(T_a) D}} \equiv f(T_a, RH) \quad (4)$$

109 where RH is the ambient relative humidity, T_a the ambient temperature, R_v the specific gas
 110 constant for water vapour, ρ liquid water density, L_v the latent heat of vaporisation, K the
 111 thermal conductivity of air, D the water vapour diffusion coefficient, and $e_s(T)$ the saturation
 112 vapor pressure at temperature T given by the Clausius-Clapeyron equation. We then define the
 113 Air Drying Capacity (ADC, in mm²/hr) as the rate of decrease of the droplet surface area:

$$114 \quad ADC(T_a, RH) \equiv -3.6 \times 8\pi \times 10^9 \times f(T_a, RH) \quad (5)$$

115 ADC is therefore an atmospheric state-variable uniquely related to air temperature and humidity
116 only. For typical ranges of air temperature and humidity, ADC varies between 0 and 15 mm²/hr
117 (Fig. 1-a,b). It is a linear function of both relative and specific humidity, but a non-linear
118 function of temperature, consistent with the Clausius-Clapeyron law. ADC strongly controls the
119 time it takes for a free-falling droplet to evaporate, and therefore the diameter cut-off between
120 “large” droplets, that reach the ground before evaporating, and “small” droplets, which turn into
121 aerosols (Fig. 1-c). At low ADC values (0-1 mm²/hr), only droplets larger than about 25µm will
122 be able to contaminate nearby surfaces, while for high ADC (>10 mm²/hr) that threshold moves
123 up to 60µm. Additionally, the potential range of such large droplets is also severely reduced as
124 ADC increases, because they can remain in the air for a significantly shorter time (Fig. 1-c, Fig.
125 S2). Small (<10µm) droplets – a size typically emitted during normal speech – while never able
126 to contaminate surfaces under the typical range of ADC values, can however potentially be
127 inhaled by subjects in the vicinity of the emitter. Their fate is largely controlled by ADC: a 10µm
128 droplet will evaporate in as much as 25s or as less as 0.5s depending on the background ADC.
129 This may be particularly relevant for VRD pathogens whose infectivity declines once in the dry
130 aerosol phase.

131

132 **Data**

133 6-hourly temperature, dew point temperature and surface pressure data at 0.75° spatial resolution
134 between 1979 and 2018 were obtained from the ERA-Interim reanalysis³⁴ (available at
135 <http://apps.ecmwf.int/datasets/>). Since ERA-Interim is only available up to 2019, we used 6-

136 hourly ERA5T³⁵ data ($0.25^\circ \times 0.25^\circ$ horizontal resolution) for the recent February-April 2020
137 period.

138 Daily COVID-19 epidemiological data compiled by the Johns Hopkins University Center for
139 Systems Science and Engineering is available at country-scale since 22 January 2020 at
140 <https://data.humdata.org/>. The most up-to-date COVID data for each US state at a daily temporal
141 resolution is taken from the COVID Tracking Project (<https://covidtracking.com/data/>).

142 Population data for world countries and US states was downloaded from
143 <https://www.worldometers.info/world-population> and <https://www.wikipedia.org>, respectively.

144 Weekly laboratory confirmed influenza cases by country for the period October 15th, 1995 to
145 August 31st, 2019 are retrieved from the World Health Organization’s FluNet database,
146 accessible at https://www.who.int/influenza/gisrs_laboratory/flunet/en/. The dataset consists in
147 weekly totals of identified influenza A and B cases, along with the number of subjects tested. It
148 suffers from both a sampling bias (variations with time and space in the number of people
149 tested), and a reporting bias (reports are not available consistently over time). We use two
150 indices of influenza prevalence to separately address these biases. First, we define an “influenza
151 frequency index”, defined weekly as the number of positive influenza A and B cases divided by
152 the number of tested subjects. Second, we define a “normalized influenza prevalence (NIP)”
153 index based on the approach of Deyle et al.¹⁴ as the number of positive cases divided by
154 population (linearly interpolated over time to account for population trends), and multiplied by
155 the average number of annual reports for all countries divided by the average number of annual
156 reports for the country in question:

$$157 \quad NIP(t, C) = \frac{\# \text{ positives, country } C, \text{ week } t}{\text{population, country } C} \times \frac{\text{avg \# weekly reports, all countries}}{\text{avg \# weekly reports, country } C}$$

158 (see supplementary methods for more details).

159

160 **Results**

161 **Climatology of ADC**

162 The spatial distribution of annual-average ADC shows a somewhat meridionally symmetric
163 pattern. The lowest values, between 0-2 mm²/hr, can be found above 60° latitude in each
164 hemisphere and over land areas around the equator (Fig. 2-a). The subtropics in each hemisphere
165 exhibit high ADC values, particularly over the large deserts of North Africa and southwest Asia
166 where temperature is high and humidity is low. Australia, India and the Western United States
167 are all characterised by relatively high ADCs. The situation during winter and spring is overall
168 quite similar, though with notable regional differences (Fig. 2-b,e). Europe and Eastern North
169 America both show particularly low ADC values during winter, much lower than in China where
170 ADC remains mostly above 2 mm²/hr. ADC over south-eastern Brazil is also at its minimum
171 (Fig. 2-e). By contrast, most of Africa, and specifically its large population centres of Ethiopia,
172 Egypt and Nigeria, all show high ADCs. The same can be said for India, particularly during
173 spring. However, consistent with the summer monsoon cycle, ADC becomes much higher during
174 and after the monsoon season over Western Africa and the Sahel region, as well as India, as
175 high-ADC bands move northwards with the rains (Fig. 2-c,d). Over Western Europe and Eastern
176 North America, ADC increases during summer, but remains rather low at around 5 mm²/hr. A
177 video showing the space-time evolution of ADC is included with Supplementary Information.

178

179 **Testing the relevance of ADC for VRD prevalence**

180 The spatial and temporal distribution of influenza cases is highly consistent with that of ADC
181 (Figs. 3-a, 4-a,b). ADC appears to set a strong upper bound on influenza prevalence that applies
182 to all countries with available data: influenza has very limited prevalence at ADCs of $5 \text{ mm}^2/\text{hr}$
183 or larger, and clearly increases as ADC approaches 0 (Figs. 3-a, 4-a,b). The annual cycles of
184 ADC and influenza are also highly consistent, with a clear peak in the disease around when ADC
185 is at its lowest (Fig. 3-c). Africa stands out due to high ADC values and low influenza
186 prevalence, whereas Europe and North America have low ADCs and generally higher numbers
187 of influenza cases (Fig. 4-a,b). While socio-economic factors also play a role in modulating the
188 spread of the disease, it is striking that ADC still constrains the upper end of the range of
189 observed prevalence, consistent with its effect on droplets – the vectors of transmission,
190 particularly the rapid increase in the time needed for droplet evaporation as ADC approaches 0
191 (Fig. S2). By contrast, air temperature (Fig. 3-b) and specific humidity (Fig. S3-a,c) do not show
192 such clear relationships to influenza, although the annual cycle of temperature appears quite
193 consistent with that of influenza prevalence (Fig. 3-d). Results for relative humidity do show
194 some enhancement of influenza as the air becomes moister (Fig. S3-b), but its annual cycle
195 seems quite off when compared to that of influenza incidence (Fig. S3-d).

196 Interestingly, the spatial distribution of ADC during winter and spring also shows some
197 resemblance to the global map of confirmed COVID-19 cases (Fig. 4-c,d, Fig. S4). The disease
198 hotspots of Europe and Eastern North America (>1000 cases per million) both have extremely
199 low ADCs, whereas China and the Western United States have fewer cases per million and larger
200 ADC, despite also being highly connected to the rest of the world. COVID-19 prevalence in
201 South America and Australia is lower (10-500 per million), and even less than that in Africa and

202 India. Naturally, many other factors come into play here, like connectivity to the rest of the
203 world, population density and localisation within countries, and public policy measures like
204 social distancing or lockdowns. The number of reported cases also suffers from biases, especially
205 undercounting. Still, countries with low (respectively high) ADCs generally seem to correspond
206 to higher (respectively lower) disease prevalence, a tendency that seems robust to considerations
207 of income levels or test numbers performed by different countries (Fig. S5).

208

209 **Discussion and Conclusions**

210 VRDs are primarily transmitted between humans through droplets exhaled by infected hosts.
211 Environmental determinants that affect the fate of these droplets can therefore influence
212 transmission of these diseases. We introduced here a new variable, ADC, motivated by droplet
213 growth theory first developed by Maxwell³². ADC includes the effects of both temperature and
214 humidity on droplet evolution in the atmosphere. Compared to temperature, ADC turns out to set
215 a much more coherent constraint on influenza prevalence (Fig. 3). The empirical relationship of
216 ADC with the average prevalence of both influenza and COVID-19 for various world regions is
217 consistent with its physical effects on the decay of droplets through which VRDs are transmitted.
218 ADC directly constrains the evaporation of airborne droplets, potentially setting a strong upper
219 bound on VRD spread and prevalence that appears valid regardless of socio-economic factor
220 (Figs. 4, S5). It is important to note that ADC also indirectly impacts the survival of liquid
221 droplets even once they have landed on surfaces; high-ADC conditions lead to rapid evaporation
222 from a surface. The transmission of the viruses responsible for COVID-19 and influenza is thus
223 likely impacted by ADC.

224 Significant relationships between temperature or humidity and influenza dynamics have been
225 suggested in previous studies for individual countries¹⁴ and temperate regions⁶, but it appears
226 that neither variable, unlike ADC, is able to explain the observed global pattern of influenza
227 prevalence (Figs. 3, S3). In particular, while specific humidity seems to have a strong effect on
228 influenza virus survival, potentially affecting its transmission during the relatively low-specific
229 humidity peak season in mid-latitude countries⁶, peak influenza in different countries occurs at
230 both times of minimum and of maximum specific humidity¹. The environmental determinant of
231 VRD proposed in this study has important implications for consistently explaining the
232 seasonality of influenza across the globe. Two kinds of favourable environments have been
233 suggested for influenza transmission: “cold-dry” (as in mid-latitude countries) and “humid-
234 rainy” (as in tropical countries),¹ in order to reconcile discrepancies in explaining seasonality of
235 influenza at the global scale.³⁶ However, if specific humidity were the determinant variable
236 impacting transmission, humid countries would hardly experience any influenza outbreaks,
237 especially during their wet season. Two clusters of high influenza prevalence can be found in the
238 WHO dataset, at both very low and very high humidity (Fig. S6). What they have in common are
239 low ADC values, and in fact each cluster corresponds to the period of annual minimum ADC in
240 mid-latitude and in tropical countries. The two proposed influenza regimes may therefore be
241 reconciled by considering ADC framework proposed in this paper. While humidity and
242 temperature may mimic influenza dynamics at the scale of individual countries,^{6,14} these same
243 relationships seem less valid when assumed for the world as whole and do not explain the large
244 discrepancies in influenza prevalence between countries. At the global scale, it appears that the

245 environment's direct effect on droplets, the VRD transmission vectors, and described here using
246 ADC, dominates over its biological effect on virus survival.

247 While ADC may only set an upper limit to VRD prevalence, social determinants like individual
248 behaviour, socioeconomic conditions, healthcare expenditure, population density, cultural norms,
249 etc. play a major role in shaping such diseases, and likely explain much of the spread in VRD
250 prevalence below the ADC-dependent threshold. Strictly speaking, ADC describes the
251 environmental conditions under which VRDs are likely to be transmitted. Whether or not
252 transmission actually occurs depends, in addition to ADC, on several complex biological as well
253 as social factors. As demonstrated in Figs. 3 and 4, the same value of ADC corresponds to a
254 range of values of observed cases of VRD. That variability in spread is undoubtedly linked to the
255 social and biologic factors independent of ADC, as well as the history of the disease in that
256 location including seeding from other locations. However, the upper limit on the observed range
257 of prevalence decreases over several orders of magnitude as ADC increases, highlighting the
258 potentially important role of this variable.

259 Variations in ADC are consistent with the explosiveness of the COVID-19 outbreak in Europe
260 and north-eastern America, where ADC is low, whereas regions with higher ADC have
261 experienced a much slower growth in cases. In particular, Africa and India stand out by high
262 ADC values and low COVID-19 prevalence (Fig. 4-a, Fig. 5). A recent study argued for a
263 reduced transmission rate in Africa potentially linked to the environment, consistent with its
264 higher ADC.⁴ Admittedly, COVID-19 data is quite limited, and very much impacted by policy
265 measures taken to limit disease spread. In addition, testing has been inconsistent across the
266 world; in many countries, reported cases largely refer to individuals showing visible symptoms

267 of the disease, leaving out many asymptomatic cases. Similarly, influenza data is not free from
268 biases (see Methods). This should make us careful in drawing final conclusions. Still, average
269 influenza and COVID-19 prevalence show a similar and consistent relationship to ADC (Fig. 3).
270 Since the high seasonality of influenza is coherent with that of ADC (Figs. 3-c), this suggests
271 that COVID-19 may also follow ADC seasonality, with potential implications for the current
272 disease hotspots of Europe and north-eastern America, where ADC will increase as summer
273 approaches (Fig. 5). In regions of Asia outside India, where the seasonality of ADC is very
274 limited, environmental determinants will probably not play much of a role in shaping COVID-19
275 dynamics in the months to come. However, the situation may be more worrying in India and
276 Western Africa, two regions where the summer monsoonal systems will bring low ADC
277 conditions offering favourable conditions for the spread of the disease if effective preventive
278 measures are not taken.

279 Nevertheless, our results present some important caveats. First, indoor heating and cooling will
280 substantially move ADC away from its outdoor value, which we considered in our analysis.
281 Transmission can occur indoors where temperature can be very different from outdoor
282 conditions. Typically, in mid-latitudes, wintertime ADC is much higher inside than outside, and
283 vice-versa during summer. Still, in regions where air conditioning and heating are available,
284 conditions indoors should tend to exhibit much less seasonality than outdoors. In addition, the
285 evident seasonality of influenza makes a strong case for the role of outdoor conditions, given that
286 people spend much of their time indoors year-round³⁶. The seasonality of VRDs may therefore
287 primarily reflect outdoor ADC.

288 Second, biological determinants of virus survival may be strongly correlated to ADC, meaning
289 that part of the ADC-VRD prevalence relationship may be explained by the effect of
290 environmental conditions on the virus itself, and not on the transmission pathway. In particular,
291 temperature is thought to affect the survival of influenza viruses⁵, though we fail to find a
292 coherent signal in global data (Fig. 3-b). Similarly, in the case of influenza and, possibly,
293 COVID-19, UV radiation is believed to be severely detrimental to viruses.⁹ Low ADC is
294 unmistakably associated with low incoming UV, but at higher levels the relationship becomes
295 less clear (Fig. S7). Therefore, ADC and UV radiation may well interact and strengthen their
296 respective effects.

297 As the COVID-19 pandemic progresses, better data will become available, and it will become
298 possible to test for the robustness of the relationship between its prevalence and ADC values. So
299 far, evidence points to an influenza-like behaviour, with a pronounced seasonality and mid-
300 latitude countries most at risk from late fall to early spring. For the latter, environmental
301 conditions will therefore probably be conducive to a second wave in late 2020, while in Western
302 Africa and India, summer 2020 may bring about favourable conditions for efficient spread of the
303 disease. However, as stressed earlier, conducive environmental conditions are not sufficient to
304 cause VRD spread, and significant outbreaks triggered by social behaviour can occur even under
305 relatively unfavourable environmental conditions.

306 **References**

- 307 1. Tamerius JD, Shaman J, Alonso WJ, et al. Environmental Predictors of Seasonal
308 Influenza Epidemics across Temperate and Tropical Climates. *PLoS Pathog* 2013; **9**:
309 e1003194.
- 310 2. Araujo MB, Naimi B. Spread of SARS-CoV-2 Coronavirus likely to be constrained by
311 climate. *medRxiv* 2020; published online Apr 7. DOI:10.1101/2020.03.12.20034728
312 (preprint).
- 313 3. Bukhari Q, Jameel Y. Will Coronavirus Pandemic Diminish by Summer? *SSRN* 2020;
314 published online Mar 17. DOI:10.2139/ssrn.3556998 (preprint).
- 315 4. Cabore JW, Karamagi H, Kipruto H, et al. The potential effects of widespread
316 community transmission of SARS-CoV-2 infection in the WHO African Region: a
317 predictive model. *BMJ global health* 2020; accepted ([https://gh.bmj.com/pages/wp-](https://gh.bmj.com/pages/wp-content/uploads/sites/58/2020/05/BMJGH-The_potential_effects_of_widespread_community_transmission_of_SARS-CoV-2_infection_in_the_WHO_African_Region_a_predictive_model-Copy.pdf)
318 [content/uploads/sites/58/2020/05/BMJGH-](https://gh.bmj.com/pages/wp-content/uploads/sites/58/2020/05/BMJGH-The_potential_effects_of_widespread_community_transmission_of_SARS-CoV-2_infection_in_the_WHO_African_Region_a_predictive_model-Copy.pdf)
319 [The_potential_effects_of_widespread_community_transmission_of_SARS-CoV-](https://gh.bmj.com/pages/wp-content/uploads/sites/58/2020/05/BMJGH-The_potential_effects_of_widespread_community_transmission_of_SARS-CoV-2_infection_in_the_WHO_African_Region_a_predictive_model-Copy.pdf)
320 [2_infection_in_the_WHO_African_Region_a_predictive_model-Copy.pdf](https://gh.bmj.com/pages/wp-content/uploads/sites/58/2020/05/BMJGH-The_potential_effects_of_widespread_community_transmission_of_SARS-CoV-2_infection_in_the_WHO_African_Region_a_predictive_model-Copy.pdf)).
- 321 5. Polozov IV., Bezrukov L, Gawrisch K, Zimmerberg J. Progressive ordering with
322 decreasing temperature of the phospholipids of influenza virus. *Nat Chem Biol* 2008; **4**:
323 248-255.
- 324 6. Shaman J, Kohn M. Absolute humidity modulates influenza survival, transmission, and
325 seasonality. *Proc Natl Acad Sci USA* 2009; **106**: 3243–3248.

- 326 7. Wang J, Tang K, Feng K, Lv W. High Temperature and High Humidity Reduce the
327 Transmission of COVID-19. *SSRN* 2020; published online Mar 10.
328 DOI:10.2139/ssrn.3551767 (preprint).
- 329 8. Chin AWH, Chu JTS, Perera MRA, et al. Stability of SARS-CoV-2 in different
330 environmental conditions. *medRxiv* 2020; published online Mar 27.
331 DOI:10.1101/2020.03.15.20036673 (preprint).
- 332 9. Sagripanti JL, Lytle CD. Inactivation of influenza virus by solar radiation. *Photochem*
333 *Photobiol* 2007; **83**: 1278–1282.
- 334 10. Homeland Security Science and Technology. Response to SARS-CoV-2 / COVID-19.
335 Apr 20, 2020. [https://www.dhs.gov/sites/default/files/publications/panthr_covid-](https://www.dhs.gov/sites/default/files/publications/panthr_covid-19_fact_sheet_v13_27apr-final_0.pdf)
336 [19_fact_sheet_v13_27apr-final_0.pdf](https://www.dhs.gov/sites/default/files/publications/panthr_covid-19_fact_sheet_v13_27apr-final_0.pdf) (accessed May 17, 2020).
- 337 11. Lowen AC, Mubareka S, Steel J, Palese P. Influenza virus transmission is dependent on
338 relative humidity and temperature. *PLoS Pathog* 2007; **3**: 1470–1476.
- 339 12. Xie X, Li Y, Chwang ATY, Ho PL, Seto WH. How far droplets can move in indoor
340 environments - revisiting the Wells evaporation-falling curve. *Indoor Air* 2007; **17**: 211–
341 25.
- 342 13. Ishmatov A. Influence of weather and seasonal variations in temperature and humidity on
343 supersaturation and enhanced deposition of submicron aerosols in the human respiratory
344 tract. *Atmos Environ* 2020; **17**: 211–25.
- 345 14. Deyle ER, Maher MC, Hernandez RD, Basu S, Sugihara G. Global environmental drivers
346 of influenza. *Proc Natl Acad Sci USA* 2016; **113**: 13081–13086.

- 347 15. Ficaretola GF, Rubolini D. Climate affects global patterns of COVID-19 early outbreak
348 dynamics. *medRxiv* 2020; published online Apr 20. DOI:10.1101/2020.03.23.20040501
349 (preprint).
- 350 16. Sajadi MM, Habibzadeh P, Vintzileos A, Shokouhi S, Miralles-Wilhelm F, Amoroso A.
351 Temperature, humidity, and latitude analysis to predict potential spread and seasonality
352 for COVID-19. *SSRN* 2020; published online Apr 6. DOI:10.2139/ssrn.3550308
353 (preprint).
- 354 17. Luo W, Majumder MS, Liu D, et al. The role of absolute humidity on transmission rates
355 of the COVID-19 outbreak. *medRxiv* 2020; published online Feb 17.
356 DOI:10.1101/2020.02.12.20022467 (preprint).
- 357 18. Poirier C, Luo W, Majumder M, et al. The Role of Environmental Factors on
358 Transmission Rates of the COVID-19 Outbreak: An Initial Assessment in Two Spatial
359 Scales. *SSRN* 2020; published online Apr 16. DOI:10.2139/ssrn.3552677 (preprint).
- 360 19. Atkinson MP, Wein LM. Quantifying the routes of transmission for pandemic influenza.
361 *Bull Math Biol* 2008; **70**: 820-867.
- 362 20. Stilianakis NI, Drossinos Y. Dynamics of infectious disease transmission by inhalable
363 respiratory droplets. *J R Soc Interface* 2010; 1355-1366.
- 364 21. Cowling BJ, Ip DKM, Fang VJ, et al. Aerosol transmission is an important mode of
365 influenza A virus spread. *Nat Commun* 2013; **4**: 1935.
- 366 22. Smieszek T, Lazzari G, Salathé M. Assessing the Dynamics and Control of Droplet- and
367 Aerosol-Transmitted Influenza Using an Indoor Positioning System. *Sci Rep* 2019; **9**:
368 2185.

- 369 23. Asadi S, Wexler AS, Cappa CD, Barreda S, Bouvier NM, Ristenpart WD. Aerosol
370 emission and superemission during human speech increase with voice loudness. *Sci Rep*
371 2019; **9**: 2348.
- 372 24. Han ZY, Weng WG, Huang QY. Characterizations of particle size distribution of the
373 droplets exhaled by sneeze. *J R Soc Interface* 2013; **10**: 20130560.
- 374 25. Wells WF. On air-borne infection: Study II. Droplets and droplet nuclei. *Am J Epidemiol*
375 1934; **20**: 611-618.
- 376 26. Bourouiba L. Turbulent Gas Clouds and Respiratory Pathogen Emissions: Potential
377 Implications for Reducing Transmission of COVID-19. *JAMA - J Am Med Assoc* 2020;
378 **323**: 1837-1838.
- 379 27. WHO. Infection prevention and control of epidemic- and pandemic-prone acute
380 respiratory infections in health care. Apr, 2014.
381 https://www.who.int/csr/bioriskreduction/infection_control/publication/en/ (accessed
382 May 17, 2020).
- 383 28. Siegel JD, Rhinehart E, Jackson M, Chiarello L. Guideline for isolation precautions:
384 Preventing transmission of infectious agents in healthcare settings. 2007.
385 <https://www.cdc.gov/infectioncontrol/guidelines/isolation/index.html> (accessed May 17.
386 2020)
- 387 29. Bourouiba L, Dehandschoewercker E, Bush JWM. Violent respiratory events: On
388 coughing and sneezing. *J Fluid Mech* 2014; **745**: 537-563.

- 389 30. WHO. Report of the WHO–China Joint Mission on Coronavirus Disease 2019 (COVID-
390 19), 16–24 Feb, 2020. [https://www.who.int/docs/default-source/coronaviruse/who-china-](https://www.who.int/docs/default-source/coronaviruse/who-china-joint-mission-on-covid-19-final-report.pdf)
391 [joint-mission-on-covid-19-final-report.pdf](https://www.who.int/docs/default-source/coronaviruse/who-china-joint-mission-on-covid-19-final-report.pdf) (accessed May 17. 2020).
- 392 31. Liu Y, Ning Z, Chen Y, et al. Aerodynamic analysis of SARS-CoV-2 in two Wuhan
393 hospitals. *Nature* 2020; published online Apr 27. DOI: 10.1038/s41586-020-2271-3
394 (preprint).
- 395 32. Maxwell JC. *The Scientific Papers of James Clerk Maxwell Vol. 1* (Dover, New York,
396 2003)
- 397 33. Rogers RR, Yau MK. *A Short Course in Cloud Physics* (Pergamon, 1989).
- 398 34. Dee DP, Uppala SM, Simmons AJ, et al. The ERA-Interim reanalysis: Configuration and
399 performance of the data assimilation system. *Q J R Meteorol Soc* 2011; **137**: 553-597.
- 400 35. Hersbach H, De Rosnay P, Bell B, et al. Operational global reanalysis: progress, future
401 directions and synergies with NWP including updates on the ERA5 production status.
402 *ERA Rep Ser* 2018. [https://www.ecmwf.int/en/elibrary/18765-operational-global-](https://www.ecmwf.int/en/elibrary/18765-operational-global-reanalysis-progress-future-directions-and-synergies-nwp)
403 [reanalysis-progress-future-directions-and-synergies-nwp](https://www.ecmwf.int/en/elibrary/18765-operational-global-reanalysis-progress-future-directions-and-synergies-nwp) (accessed May 17. 2020).
- 404 36. Tamerius J, Nelson MI, Zhou SZ, Viboud C, Miller MA, Alonso WJ. Global influenza
405 seasonality: Reconciling patterns across temperate and tropical regions. *Environ Health*
406 *Perspect* 2011; **119**: 439-445.
- 407 37. Effros, R. M. et al. Dilution of respiratory solutes in exhaled condensates. *Am. J. Respir.*
408 *Crit. Care Med.* 2002 **165**: 663–669.

409 **Author Contributions**

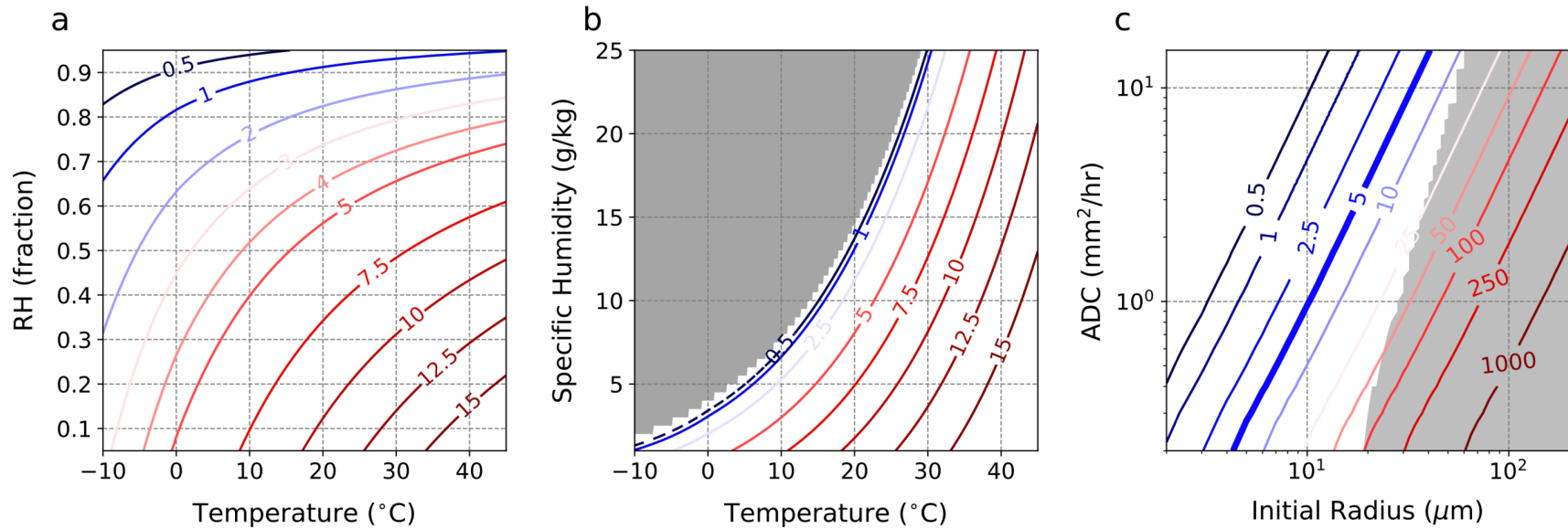
410 E. A. B. E. devised and supervised the study. Y. C. and A. T. carried out analyses. All authors
411 contributed to the manuscript.

412 **Competing Interests**

413 The authors declare that they have no competing financial interests.

414 **Correspondence**

415 Correspondence and requests for materials should be addressed to atuel@mit.edu.



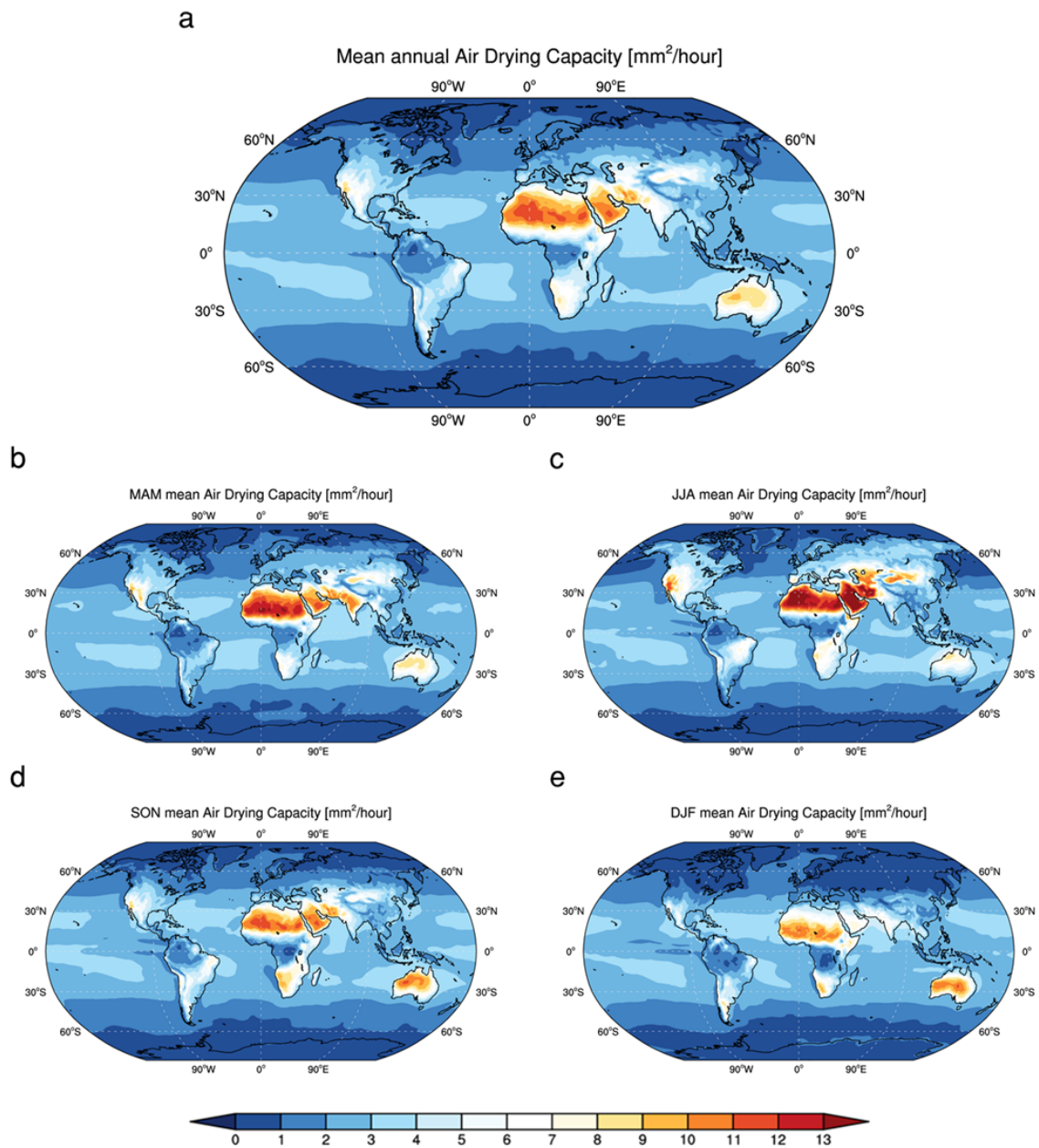
416

417 Figure 1. **ADC and environmental conditions.** (a-b) Air Drying Capacity (ADC, unit: mm²/hour) as a function of temperature and

418 (a) relative humidity and (b) specific humidity. The grey area in (b) indicates super-saturation. (c) Time to evaporation of free-falling,

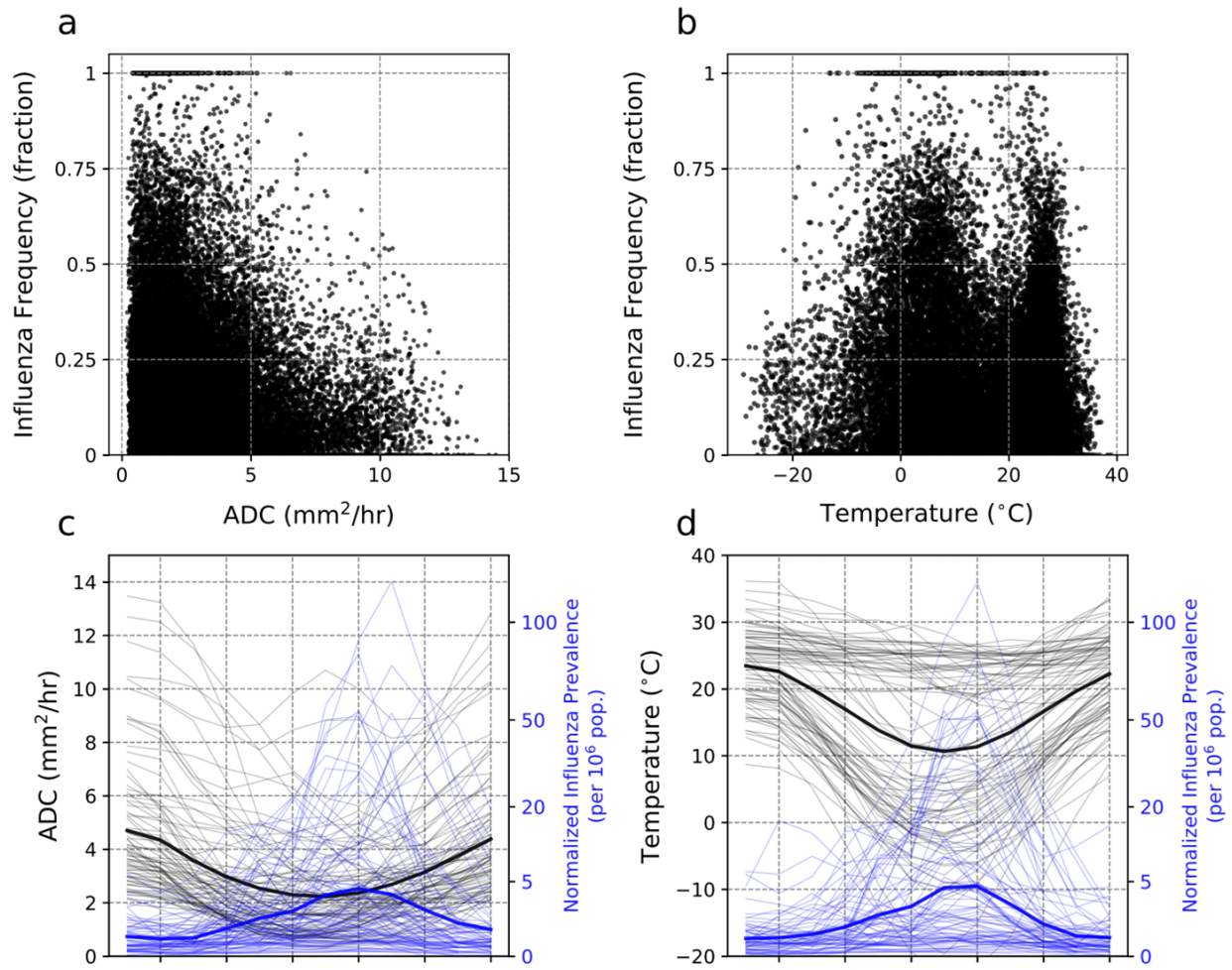
419 spherical water droplets as a function of ADC and initial droplet radius. The shaded area indicate the region where droplets reach the

420 ground before evaporating.



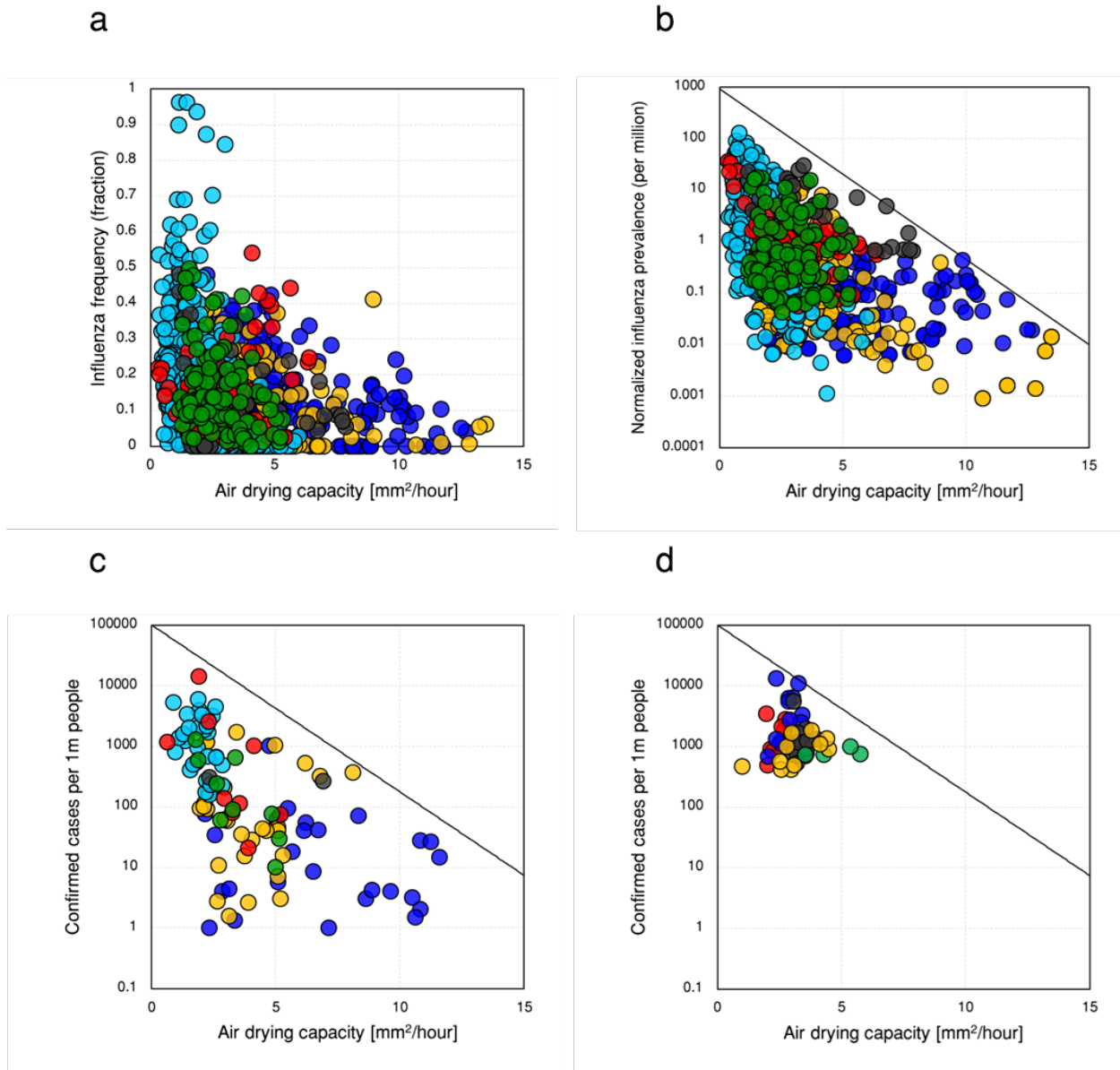
421

422 Figure 2. **Global distribution of ADC.** (a-e) Global map of (a) annual, (b) spring (March to
 423 May), (c) summer (June to August), (d) autumn (September to November), and (e) winter
 424 (December to February) average ADC for the period 1979-2018, calculated from the ERA-
 425 Interim dataset.



426

427 **Figure 3. Seasonal variation of ADC and prevalence of VRD.** (a-b) Weekly influenza
 428 frequency against (a) ADC and (b) temperature. (c-d) Seasonal variation of normalised influenza
 429 prevalence alongside (c) ADC and (d) temperature. In (c-d), the first month is defined for each of
 430 the 85 countries as the month with maximum ADC (c) or temperature (d).



431

432 **Figure 4. ADC and viral respiratory disease (VRD) prevalence.** (a-b) Long-term monthly-
 433 mean ADC against long-term monthly-mean (a) influenza A and B frequency, and (b)

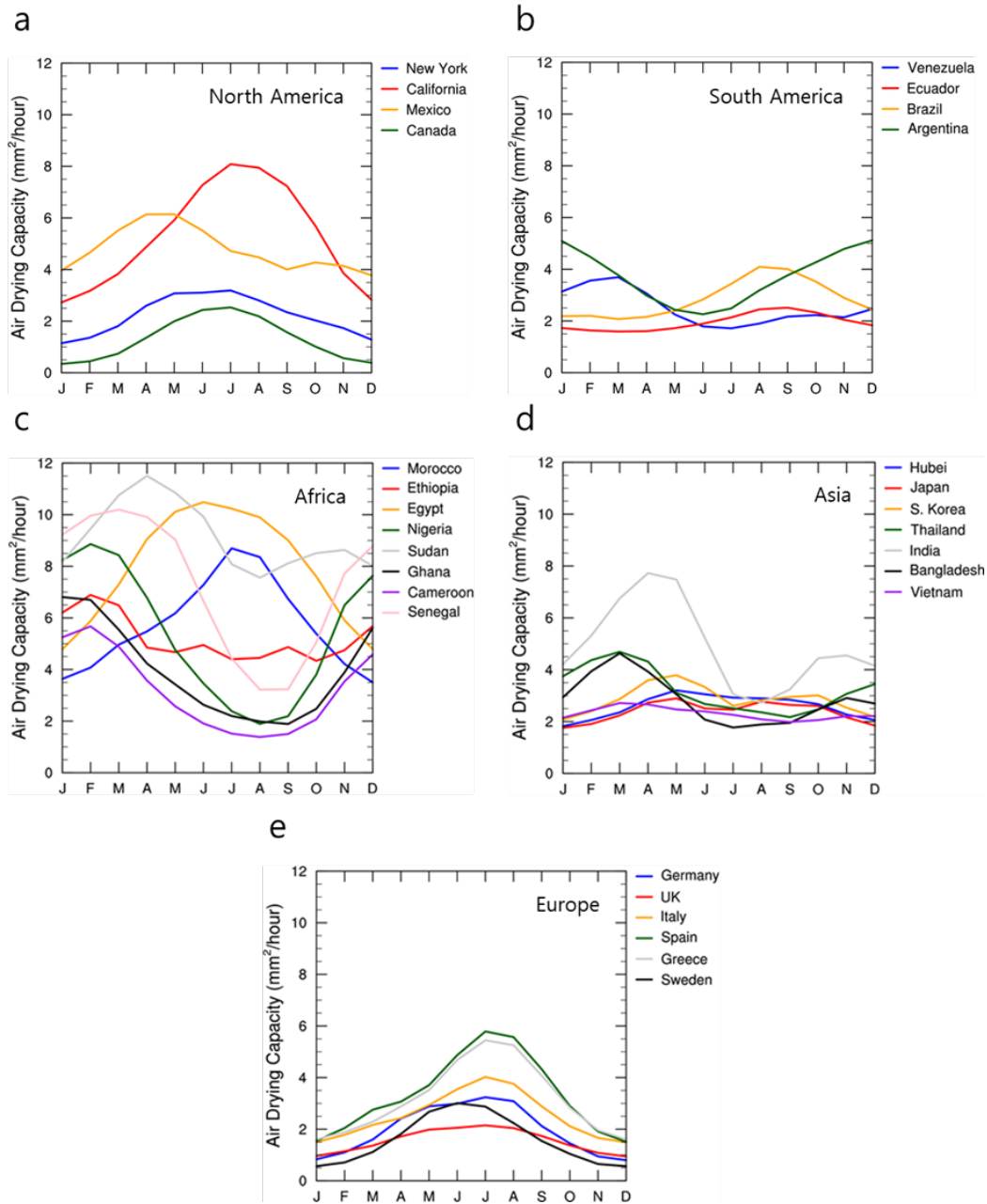
434 normalized influenza prevalence for 85 countries (Table S1) for the 1995-2019 period. (c)

435 February-April 2020 ADC against concurrent accumulated confirmed COVID-19 cases for 108

436 countries (Table S1). (d) Same as (c), but for the 50 US states. Red, green, light blue, yellow,

437 blue and black colors in (a,b,c) respectively indicate North America, South America, Europe,

438 Asia, Africa, and Oceania countries, and in (d) the Western, North-eastern, Midwestern, South-
439 eastern, and South-western US states are represented by yellow, blue, red, black, and green
440 colours, respectively.



441
 442 Figure 5. **Seasonal variations of ADC.** (a-e) Monthly seasonal cycle of ADC for (a) North
 443 America, (b) South America, (c) Africa, (d) Asia, and (e) Europe. Data from 6-hourly ERA-
 444 Interim reanalysis.